

Andreev Bound states as a phase sensitive probe of the pairing symmetry of the iron pnictide superconductors.

Pouyan Ghaemi,¹ Fa Wang,^{1,2} and Ashvin Vishwanath^{1,2}

¹*Department of Physics, University of California at Berkeley, Berkeley, CA 94720*

²*Materials Sciences Division, Lawrence Berkeley National Laboratory, Berkeley, CA 94720*

(Dated: November 3, 2018)

A leading contender for the pairing symmetry in the Fe-pnictide high temperature superconductors is extended s-wave s_{\pm} , a nodeless state in which the pairing changes sign between Fermi surfaces. Verifying such a pairing symmetry requires a special phase sensitive probe that is also momentum selective. We show that the sign structure of s_{\pm} pairing can lead to surface Andreev bound states at the sample edge. In the clean limit they only occur when the edge is along the nearest neighbor Fe-Fe bond, but not for a diagonal edge or a surface orthogonal to the c-axis. In contrast to d-wave Andreev bound states, they are not at zero energy and, in general, do not produce a zero bias tunneling peak. Consequences for tunneling measurements are derived, within a simplified two band model and also for a more realistic five band model.

PACS numbers:

Central to the physics of the recently discovered iron pnictide superconductors, is the nature of the pairing symmetry. Given the high transition temperatures and proximity to a magnetically ordered state, a non-phonon mechanism is indicated. Hence, unconventional pairing symmetry, as often occurs in other such cases like the cuprates, organic conductors and heavy fermion materials, is to be expected. Current theories predict a wide variety of possible pairing states, ranging from p-wave^{1,2} to d-wave^{3,4}, and also extended s-wave s_{\pm} , a nodeless pairing state where the pairing changes sign between different Fermi pockets^{5,6,7,8}. The last is a theoretically attractive candidate since it is a naturally connected with the magnetic order observed in the undoped parent materials^{6,7,8,9}. While initial experimental results seemed to favor a pairing state with nodes in the gap function, recently, the bulk of the experimental evidence has been in favor of a completely gapped state. For example, ARPES experiments¹⁰ see a full gap around all Fermi pockets, and recent specific heat measurements are consistent with the absence of nodes¹¹. The extended s-wave state is therefore emerging as an strong candidate for the pairing symmetry. Hence, it is important to consider experimental tests that can directly probe such a state. In contrast to the d-wave symmetry of the cuprates, which changes sign under rotation and hence can be probed by a class of phase sensitive experiments¹², the sign change in the s_{\pm} state is not accessible by a real space transformation. Instead, as shown in figure 1(a), the pairing phase changes on moving across the Brillouin zone. Probing such a sign change is a much more challenging task. A parametrization of the pairing function that gives this sign structure on the fermi surfaces is $\Delta(k_x, k_y) = \Delta_0 \cos k_x \cos k_y$ ⁹, where (k_x, k_y) represents the crystal momentum along the Fe-Fe bonds. The pairing changes sign on crossing the $k_x = \pm\pi/2$ and $k_y = \pm\pi/2$ lines. It is this sign change that we wish to probe.

An interesting consequence of *d-wave* pairing in the

cuprates is the presence of Andreev bound states at the edge which leads to a zero-bias peak in conductivity in superconductor/normal junctions^{13,14,15}. The existence of these modes can be intuitively understood as follows. Consider an electron with momentum k incident on a surface, where it is reflected to momentum k' . When the pairing function changes sign in this process $\Delta(k)/\Delta(k') < 0$, then the problem is related to a superconductor-normal-superconductor junction with a relative phase shift of π . There it is well known that a midgap state arises near the chemical potential¹⁶. This leads to Andreev bound states along those edges of the d-wave superconductor that reflect particles in the sign reversed way described above. Note, the Andreev bound states reach all the way down to the chemical potential (zero energy), and hence are experimentally detected as a zero bias peak in tunneling measurements^{13,14}. The dependence on edge orientation can be erased in samples with disordered surfaces. Nevertheless, in some cases a strong experimental difference has been observed between 45° rotated a-b plane edges¹⁵. The zero bias anomaly does not arise in c-axis tunneling, as predicted.

In this letter we study the surface Andreev bound states at the edge of an extended s-wave superconductor. Although our results are more general, we focus on the models proposed for the pnictide superconductors. By the intuitive argument described above, we expect that when an electron is scattered by the edge between Fermi pockets with opposite sign of pairing, Andreev bound states should result. We indeed find this to be the case, in the microscopic models that we study, but with one important distinction from the d-wave case. The spectrum of Andreev bound states within the bulk gap does not reach down to zero energy. A zero bias tunneling anomaly is hence not expected. Nevertheless, the presence of these Andreev modes will lead to peaks in the tunneling current within the bulk gap, which should be observable. From figure 1(a), it is seen that scattering between Fermi surfaces with opposite sign of pairing oc-

curs for an edge parallel to the nearest neighbor Fe-Fe bond (along the [100] or [010] directions) but not for the diagonal edge ([110] direction) or the c-axis edge ([001] direction - we assume negligible c-axis dispersion). Indeed, we only find bound Andreev states for the expected edge directions, and these disappear if the relative sign of pairing is removed (i.e. with regular s-wave pairing). The sensitivity to edge orientation is a key signature of these Andreev surface states. At present, tunneling experiments on the Fe-pnictide superconductors are restricted to polycrystalline samples¹⁷, which makes comparison to theory difficult. Tunneling experiments on single crystals can unambiguously identify these states.

We study two microscopic models of the Fe pnictides. The first is a simplified two band model^{18,19}, in which the Andreev bound states can be studied analytically. The Andreev bound state energy is found to be controlled by the overlap between the Bloch wavefunctions of the incident and scattered electronic states, and satisfies the intuitive requirement that as the wavefunction overlap decreases, the in-gap state approaches the continuum. With increasing overlap, the bound state approaches zero energy, which is achieved if the overlap is perfect. A typical choice of parameters yields a dispersing in-gap mode whose minimum energy is less than 50% of the bulk gap. Since the two band model differs in some subtle but important respects from the LDA determined band structures¹, we have also studied a more realistic five-band tight binding model²⁰. Here we find qualitatively similar results. For the particular doping that we study in detail, the in-gap state is at a higher energy, 92% of the bulk gap at that edge momentum. Since a perfectly smooth edge is hard to realize experimentally, we model edge roughness by allowing for orbital mixing during scattering (but preserve the edge momentum quantum number). Within this crude model of a rough edge, the in-gap states occur at much lower energy (eg. 50% of the bulk gap value). Observable signatures in experiments with planar and point contact tunnel junctions are discussed. In the treatment below, we solve the Bogoliubov-deGennes equations for superconductor quasiparticles near the sample edge, with a uniform pairing potential. For weak coupling superconductors, the pair potential is to be calculated self consistently, which we do not do here. A self consistent solution is expected to lead to a smaller pairing potential near the edge, due to the presence of in-gap states. This is not expected to change our results qualitatively, and moreover, it is not even clear if such weak coupling reasoning is justified for these high temperature superconductors.

Two Band Model: We first present the study of the two band model for pnictides at half filling. The details of this model could be found elsewhere¹⁸. The band Hamiltonian we consider in momentum space has the form:

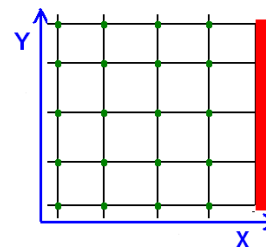
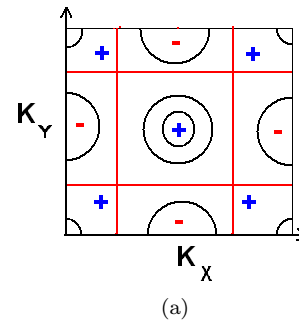


FIG. 1: a) Fermi surfaces of Fe pnictides and extended s-wave pairing sign in the unfolded Brillouin zone b) Real space square lattice of iron atoms and the [100] boundary (red)

$$H = H_0 + H_\Delta \quad (1)$$

$$H_0 = \sum_{\mathbf{k}} \begin{pmatrix} d_{1,\mathbf{k},\sigma}^\dagger & d_{2,\mathbf{k},\sigma}^\dagger \end{pmatrix} K(\mathbf{k}) \begin{pmatrix} d_{1,\mathbf{k},\sigma} \\ d_{2,\mathbf{k},\sigma} \end{pmatrix} \quad (2)$$

$$H_\Delta = \sum_{\mathbf{r},\mathbf{r}'} \epsilon_{\sigma,\sigma'} \delta_{a,b} \left[d_{a,\mathbf{r},\sigma}^\dagger d_{b,\mathbf{r}',\sigma'}^\dagger \right] + H.c. \quad (3)$$

where $d_1(d_2)$ represents $3d_{xz}(3d_{yz})$ orbitals of Iron, ϵ is the 2×2 antisymmetric matrix and σ is the spin index. The momentum sum is over the enlarged Brillouin zone $k_x \in [-\pi, \pi)$, $k_y \in [-\pi, \pi)$. The 2×2 matrix $K(\mathbf{k})$ in Ref.¹⁹, after rotation into the $d_{xz,yz}$ basis is:

$$K(k_x, k_y) = 2t_1(\cos k_x - \cos k_y)\tau_3 + 2(t_2 - t'_2) \sin k_x \sin k_y \tau_1 + [2(t_2 + t'_2) \cos k_x \cos k_y + 2t'_1(\cos k_x + \cos k_y)] \cdot I \quad (4)$$

and $\tau_{1,2,3}$ are Pauli matrices and I is the identity matrix. Here we present the numerical results for $t_1 = 1eV, t_2 = 1.7eV$ and $t'_1 = t'_2 = 0$ at zero doping¹⁹.

We numerically diagonalize a 600 site wide lattice, with an edge along the [100] direction. The momentum k_{\parallel} along this direction is conserved and used to label the eigenstates. Interestingly we see (Figure 2) that a dispersing mid-gap state is obtained, with energy as low as 39% of the bulk gap. This is the Andreev surface bound state. For convenience, we work with a bulk gap of 46 meV which is a few times larger the experimentally

measured gap. We have checked that the energy of the mid-gap features scale linearly with the gap size over a wide range hence our results hold when scaled with the bulk gap. The results were also compared against those obtained from transfer matrix method²¹ which does not suffer from finite size errors. The dispersing mode leads to a feature in the density of states (Figure 2 inset), which could potentially be detected in the tunneling experiments. No surface Andreev states are obtained with the edge along the [110] direction, or if an onsite s-wave pairing, with uniform sign in momentum space is used.

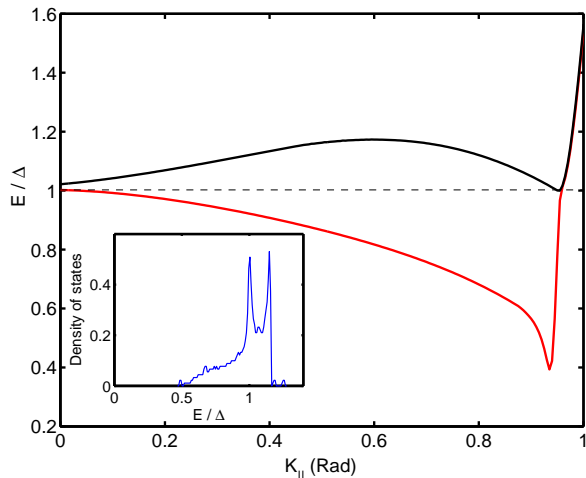


FIG. 2: Dispersion of Andreev bound states (red) and the bottom of the continuum (black) as a function of k_{\parallel} , the momentum parallel to the edge. Energy is scaled by Δ , the minimum energy gap in the bulk. Inset shows the density of states integrated over k_{\parallel} .

In the two band model, one feature of the edge mode as can be seen in figure 2, is that at transverse momentum $k_{\parallel} = 0$ the edge mode merges with the continuum. This arises because the Bloch wavefunctions on the electron and hole pockets at $k_{\parallel} = 0$ are orthogonal (they have opposite eigenvalues under reflection). Hence, the gap sign changing scattering is forbidden, and no surface Andreev state appears. On moving away from this special momentum, the scattering is allowed, leading to Andreev bound state. Our analytical treatment below captures the relation between wavefunction overlap and Andreev bound state energy.

We now analytically demonstrate the presence of edge modes as a result of change of sign of order parameter on the two Fermi surfaces in the two band model. For each value of k_{\parallel} , the momentum parallel to the edge, we have a one dimensional Hamiltonian. The low energy excitations occur close to the Fermi points, labeled as left mover and right movers (fig. 3) for each Fermi pocket. The low energy electronic field $\Psi_{\sigma}(x)$ written as a two component object to account for the two orbitals, can be expanded as $\Psi_{\sigma}(x) = \sum_n \psi_{Rn\sigma}(x) \mathbf{u}_n^R e^{ik_{fn}x} + \psi_{Ln\sigma}(x) \mathbf{u}_n^L e^{-ik_{fn}x}$, where n labels different Fermi pockets, σ labels physical spin (we suppress k_{\parallel} index from now on for simplicity)

and $\mathbf{u}_n^{R/L}$ are the two component Bloch wave functions at the Fermi points.



FIG. 3: Effective one dimensional model of the two band Hamiltonian, at a fixed k_{\parallel} . Low energy excitations are labeled as right (R) and left (L) movers. Hole (electron) Fermi pockets are shown in green (red).

In these variables, the superconducting Hamiltonian is:

$$H = \int dx \sum_{n=1}^2 \left[\left(\psi_{nR\uparrow}^{\dagger}, \psi_{nL\downarrow} \right) \begin{pmatrix} -iv_n \partial_x & \Delta_{nR} \\ \Delta_{nR}^* & iv_n \partial_x \end{pmatrix} \begin{pmatrix} \psi_{nR\uparrow} \\ \psi_{nL\downarrow}^{\dagger} \end{pmatrix} + \left(\psi_{nL\uparrow}^{\dagger}, \psi_{nR\downarrow} \right) \begin{pmatrix} iv_n \partial_x & \Delta_{nL} \\ \Delta_{nL}^* & -iv_n \partial_x \end{pmatrix} \begin{pmatrix} \psi_{nL\uparrow} \\ \psi_{nR\downarrow}^{\dagger} \end{pmatrix} \right] \quad (5)$$

Here $n = 1, 2$ are the hole and electron pockets, while v_n labels the fermi velocity and Δ_n is the superconducting gap on the n 'th fermi pocket.

We are looking for a localized solution on the edge and consider the following ansatz to represent the edge mode which diagonalize Hamiltonian 5:

$$\Phi_1 = \sum_n \int dx e^{-\frac{x}{\lambda_n} + ik_{fn}x} \left(\alpha_{nR\uparrow} \psi_{nR\uparrow}(x) \mathbf{u}_n^R + \alpha_{nL\downarrow}^* \psi_{nL\downarrow}^{\dagger}(x) \mathbf{u}_n^{L*} \right) \\ \Phi_2 = \sum_n \int dx e^{-\frac{x}{\lambda_n} - ik_{fn}x} \left(\alpha_{nR\downarrow}^* \psi_{nR\downarrow}^{\dagger}(x) \mathbf{u}_n^{R*} + \alpha_{nL\uparrow} \psi_{nL\uparrow}(x) \mathbf{u}_n^L \right)$$

They satisfy $[\Phi, H] = E \Phi$ with $E < \Delta$ which leads to BdG equations for α 's. At the boundary the particle and hole amplitude should separately vanish²². This leads to the following boundary equation:

$$\sum_n c_{1n} \mathbf{u}_n^R \alpha_{nR\uparrow} + c_{2n} \mathbf{u}_n^L \alpha_{nL\uparrow} = 0 \quad (6)$$

$$\sum_n c_{2n} \mathbf{u}_n^{R*} \alpha_{nR\downarrow}^* + c_{1n} \mathbf{u}_n^{L*} \alpha_{nL\downarrow}^* = 0 \quad (7)$$

These are set of equations for c 's. The condition for existence of non-zero solution for c determines the bound state energy. The Bloch function on the two fermi surfaces can then be chosen to have the simple form: $\mathbf{u}_1^R = (r_1, s_1)^T$, $\mathbf{u}_1^L = (-r_1, s_1)^T$, $\mathbf{u}_2^R = (r_2, s_2)^T$ and $\mathbf{u}_2^L = (-r_2, s_2)^T$. We can solve the BdG equations for the bound state in general, regardless of magnitude of

gap on the fermi surfaces but the expressions are greatly simplified if we assume that $|\Delta_1| = |\Delta_2| = \Delta$. We present the result for this case here. When $\Delta_1\Delta_2 < 0$ we get a pair of bound states related by time reversal symmetry with energy:

$$E = \pm \Delta \left| \frac{s_2^* r_1 + r_2^* s_1}{s_2 r_1 - r_2 s_1} \right| \quad (8)$$

Notice the energy of these states is related to the orbital structure on two fermi surfaces. With real wavefunctions, these states occur within the bulk gap if $r_1 s_1 r_2 s_2 < 0$, which is satisfied in the two band model of Eq. 4. Only with complete orbital overlap of \mathbf{u}_1^R and \mathbf{u}_2^L are they at zero energy. On the other hand, when the gaps have the same sign (i.e. $\Delta_1 = \Delta_2 = \Delta$), no localized mode is found as expected.

Five band model: We also preformed a numerical study of a more realistic five band model²⁰ at 18% electron doping. We again consider a Hamiltonian of the form (2), but $d_{\mathbf{k},\sigma}$ are now five component spinors. The detailed form of $K(\mathbf{k})$ is given in ref. 20. Superconducting pairing is as in Eqn. 3, but now with five orbitals. We performed exact diagonalization on lattices 600 sites wide with a [100] edge. While we do not present a general analytical solution to the five band model edge modes due to its complexity, we have verified that at $k_{\parallel} = 0$, where the problem simplifies, the mid-gap state is obtained.

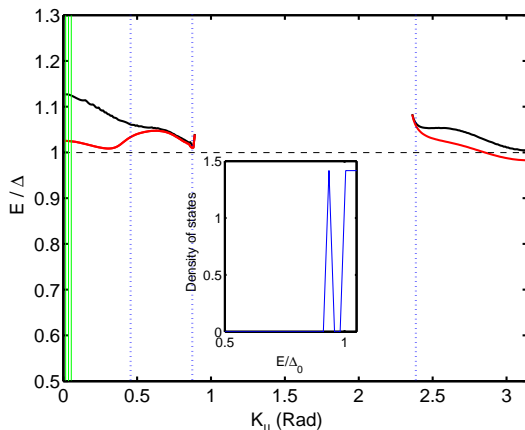


FIG. 4: Andreev bound state dispersion (red) and bottom of continuum (black). Inset presents the density of states for transverse momenta near $k_{\parallel} = 0$ (green region). Dotted lines denote the positions of fermi surfaces

The dispersion of edge mode as a function of transverse momentum is shown in Fig. 4. Although Andreev bound states are present, in this case they happen to be close to the continuum. Around $k_{\parallel} = 0$ the Andreev bound state is at 92% of the bottom of the continuum for that momentum. Note, the precise value of the edge mode energies depend sensitively on the band structure details, as well as on doping. Hence, the main value of this result is in establishing the existence of the Andreev

bound states in the five band model as well. Moreover they also occur for $k_{\parallel} = 0$, since the wavefunction overlap is nonvanishing at that point, in contrast to the two band model. In the inset of Fig. 4, the density of states near $k_{\parallel} = 0$ is shown in units of $[eV]^{-1}$ per unit-cell. This may in principle be probed by planar junction tunneling, which probes excitations in a small momentum cone.

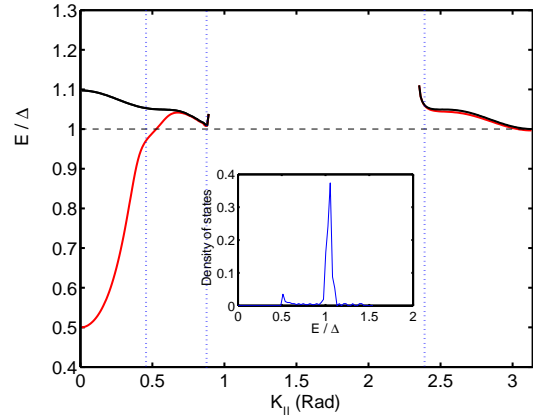


FIG. 5: Dispersion of in-gap mode (red) and bottom of continuum (black) after adding a perturbing potential on the edge. Inset present the density of states. Dotted lines denotes the position of Fermi surfaces

Up to here, we have only considered a clean edge, but this is not always the case in a realistic experimental setting. From our analytical treatment it is clear that the energy of the edge mode depends on the orbital structure on the two fermi surfaces and so indeed any (non-magnetic) perturbing potential that mixes the orbitals on the edge can change this mid-gap energy. In Fig. 5 we present one example of the dispersion of mid-gap states when we have an impurity potential on the edge which transforms the orbital structure of one fermi surface to the other. Guided by this expectation we choose the following potential on the edge. We choose an impurity potential on the boundary ($x = 0$) of the form $H_{imp} = 0.3\delta_{x,0}[\mathbf{u}_1^R \otimes \mathbf{u}_2^L + h.c.]$ where \mathbf{u}_1^R and \mathbf{u}_2^L denote the Bloch wave functions for the electrons on the small hole Fermi surface, and the electron Fermi surface respectively at $k_{\parallel} = 0$, in a gauge where they are purely real. The bound states now reach down to about 50% of the bulk gap as shown in Figure 5. For technical reasons, we do not consider the most general impurity potential that would break translation symmetry along the edge and hence we still retain the momentum k_{\parallel} .

Conclusions: In this letter we have shown the presence of Andreev bound state on the surface of a superconductor with extended s-wave pairing, which are strongly sensitive to surface orientation. In contrast to d-wave Andreev bound states, they are typically at a finite energy. Although the bound state energy is hard to predict reliably, since it depends in detail on the orbital structure of Bloch wave functions on the fermi surfaces with anti-phase paring, the states were found to occur in different

microscopic models of the Fe-pnictides with extended s-wave pairing. Tunneling experiments on a-b plane edges with planar or point contacts, or even STM on step edges can potentially detect these states which, if observed, will

be an important step to establishing the pairing symmetry in these materials. We thank Dung-Hai Lee for instructive discussions. We acknowledge support from LBNL DOE-504108.

-
- ¹ P. A. Lee and X.-G. Wen, Phys. Rev. B **78**, 144517 (2008).
² X.-L. Qi, S. Raghu, C.-X. Liu, D. J. Scalapino, and S.-C. Zhang (2008), arXiv:0804.4332.
³ Z.-J. Yao, J.-X. Li, and Z. D. Wang (2008), arXiv:0804.4166.
⁴ Q. Si and E. Abrahams, Phys. Rev. Lett. **101**, 076401 (2008).
⁵ I. I. Mazin, D. J. Singh, M. D. Johannes, and M. H. Du, Phys. Rev. Lett. **101**, 057003 (2008).
⁶ A. V. Chubukov, D. V. Efremov, and I. Eremin, Phys. Rev. B **78**, 134512 (2008).
⁷ F. Wang, H. Zhai, Y. Ran, A. Vishwanath, and D.-H. Lee (2008), arXiv:0807.0498.
⁸ H. Zhai, F. Wang, and D.-H. Lee (2008), arXiv:0810.2320.
⁹ K. Seo, B. A. Bernevig, and J. Hu, Phys. Rev. Lett. **101**, 206404 (2008).
¹⁰ H.-Y. Liu, X.-W. Jia, W.-T. Zhang, L. Zhao, J.-Q. Meng, G.-D. Liu, X.-L. Dong, G. Wu, R.-H. Liu, X.-H. Chen, et al., Chin. Phys. Lett. **25**, 3761 (2008).
¹¹ G. Mu, H. Luo, Z. Wang, L. Shan, C. Ren, and H.-H. Wen (2008), arXiv:0808.2941.
¹² D. A. Wollman, D. V. Harlingen, W. C. Lee, , D. M. Ginsberg, and A. J. Leggett, Phys. Rev. Lett. **71**, 2134 (1993).
¹³ S. Kashiwaya, Y. Tanaka, M. Koyanagi, H. Takashima, and K. Kajimura, Phys. Rev. B **51**, 1350 (1995).
¹⁴ M. Covington, M. Aprili, E. Paraoanu, L. H. Greene, F. Xu, J. Zhu, and C. Mirkin, Phys. Rev. Lett. **79**, 277 (1997).
¹⁵ L. H. Greene et al., Physica C: Superconductivity **387**, 162 (2003).
¹⁶ A. M. Zagorkin and H. E. Stanley, *Quantum Theory of Many-Body Systems* (Springer, 1998).
¹⁷ T. Y. Chen, Z. Tesanovic, R. H. Liu, X. H. Chen, and C. L. Chien, Nature **453**, 1224 (2008).
¹⁸ S. Raghu, X.-L. Qi, C.-X. Liu, D. Scalapino, and S.-C. Zhang, Phys. Rev. B **77**, 220503 (2008).
¹⁹ Y. Ran, F. Wang, H. Zhai, A. Vishwanath, and D.-H. Lee (2008), arXiv:0805.3535.
²⁰ K. Kuroki, S. Onari, R. Arita, H. Usui, Y. Tanaka, H. Kontani, and H. Aoki, Phys. Rev. Lett. **101**, 087004 (2008).
²¹ D. H. Lee and J. D. Joannopoulos, Phys. Rev. B **23**, 4988 (1981).
²² C.-R. Hu, Phys. Rev. Lett. **72**, 1526 (1994).